STEM CELLS®

REGENERATIVE MEDICINE

Transplantation of Mesenchymal Stem Cells Promotes Tissue Regeneration in a Glaucoma Model through Laser-induced Paracrine Factor Secretion and Progenitor Cell Recruitment

Renaud Manuguerra-Gagné,[1,2,5] Patrick R. Boulos,[2,3] Ahmed Ammar,[1,2], François A. Leblond,[4] Gorazd Krosl,[1] Vincent Pichette,[4,5,6] Mark R. Lesk[2,3,5] and Denis-Claude Roy[1,5]

Division of [1]Hematology-Oncology and [4]Nephrology, Hopital Maisonneuve-Rosemont Research Center, Montreal, Canada; [2] Department of Vision Health Research, Hopital Maisonneuve-Rosemont, Montreal, Canada; [3]Department of Ophthalmology, University of Montreal, Montreal, Canada; Department of [5]Medicine and [6]Pharmacology, University of Montreal, Montreal, Canada

Key words. Tissue regeneration • bone marrow mononuclear cells • mesenchymal stem cells • glaucoma • intraocular pressure

ABSTRACT

Among bone marrow cells, hematopoietic and mesenchymal components can contribute to repair damaged organs. Such cells are usually used in acute diseases but few options are available for the treatment of chronic disorders. In the present study, we have used a laser-induced model of open angle glaucoma (OAG) to evaluate the potential of bone marrow cell populations and the mechanisms involved in tissue repair. In addition, we investigated laser-induced tissue remodeling as a method of targeting effector cells into damaged tissues. We demonstrate that among bone marrow cells, mesenchymal stem cells (MSC) induce trabecular meshwork (TM) regeneration. MSC injection into the ocular anterior chamber lead to far more efficient decrease in intraocular pressure (IOP) ($P<0.001$) and healing than hematopoietic cells. This robust effect was attributable to paracrine factors from stressed MSC, as injection of conditioned medium from MSC exposed to low but not to normal oxygen levels resulted in an immediate decrease in IOP. Moreover, MSC and their secreted factors induced reactivation of a progenitor cell pool found in the ciliary body and increased cellular proliferation. Proliferating cells were observed within the chamber angle for at least 1 month. Laser-induced remodeling was able to target MSC to damaged areas with ensuing specific increases in ocular progenitor cells. Thus, our results identify MSC and their secretum as crucial mediators of tissue repair in OAG through reactivation of local neural progenitors. In addition, laser treatment could represent an appealing strategy to promote MSC-mediated progenitor cell recruitment and tissue repair in chronic diseases.

INTRODUCTION

Author contributions: R.M.-G.: Conception and design, collection and/or assembly of data, data analysis and interpretation, manuscript writing; P.R.B.: Conception and design; A.A.: Conception and design, collection and/or assembly of data; F.A.L.: Conception and design, collection and/or assembly of data; G.K.: Conception and design, manuscript writing; V.P.: Conception and design; M.R.L.: Conception and design, administrative support, financial support, manuscript writing; D.-C.R.: Conception and design, administrative support, financial support, manuscript writing

Corresponding Authors: Denis Claude Roy, MD, Cellular Therapy Laboratory, Hospital Maisonneuve-Rosemont Research Center, 5415 l'Assomption blvd., Montreal, Quebec, H1T 2M4, Canada, Telephone; 514-252-3400 ext 3331, Fax; 514-252-3430, Email; denis-claude.roy@umontreal.ca; Mark Lesk, MSc.,MD, Glaucoma Research Laboratory, Hopital Maisonneuve-Rosemont Research Center, 5415 l'Assomption blvd., Montreal, Quebec, H1T 2M4, Canada, Telephone; 514-252-3400 ext 4959, Fax; 514-251-7094, Email; lesk@videotron.ca; Supported by Glaucoma Research Society of Canada, Thécell Network – Fonds Recherche Quebec – Sante (FRQS), Fonds de Recherche en Ophtalmologie de l'Université de Montréal, the Fonds de recherche Québec - Santé, and Canadian Institutes for Health Research; Received July 07, 2012; accepted for publication February 05, 2013; 1066-5099/2013/$30.00/0 doi: 10.1002/stem.1364

This article has been accepted for publication and undergone full peer review but has not been through the copyediting, typesetting, pagination and proofreading process which may lead to differences between this version and the Version of Record. Please cite this article as doi: 10.1002/stem.1364

One of the most important breakthroughs of the last decade is the discovery that stem cells from various tissues have the ability to repair damaged organs. However, the repair mechanisms used by such cells are only beginning to be elucidated. Such effects can be mediated by undifferentiated stem cells transforming into mature cells with specialized function [1-4]. Alternatively, stem cells could also secrete cytokines and other factors that enhance intrinsic repair mechanisms and promote the development of a protective environment capable of changing the outcome for cells that have sustained potentially lethal damage [5-10]. Experimental data support immune modulation and neovascularization as mechanisms, but few other pathways have been thoroughly investigated [11-14]. In addition, it has been shown that stem cells are particularly active when injected soon after the initiation of acute tissue damage or in the presence of active disease [10, 15, 16]. In chronic disorders or instances where scarring has already developed, decreased homing signals and release of cytokines within dysfunctional or fibrotic tissues may limit the efficacy of cellular interventions. Thus, there is a dire need to develop approaches to create space and enhance stem cell recruitment to such tissues.

Among the various organs targeted by cellular interventions, the eye offers particularly attractive features to rapidly advance cell therapy [17]. Indeed the eye is immediately accessible for cellular injection, and allows rapid as well as direct visualization and monitoring of the impact of therapeutic interventions. One of the most important chronic optic neuropathies and an important cause of blindness worldwide is open angle glaucoma (OAG [18]). It is primarily associated with increased resistance to the outflow of aqueous humor through the trabecular meshwork (TM) resulting from apoptotic cell loss and subsequent increase in extracellular matrix density [19-25]. Elevated intraocular pressure (IOP) is the most important risk factor for glaucoma, as changes in IOP homeostasis can result in damage to the optic nerve, and reduction of IOP is the mainstay of therapy [26, 27]. Treatments include life-long medication to lower the production of aqueous humor, laser treatment of the TM to temporarily help regulate IOP, or invasive surgical procedures to allow aqueous humor outflow through alternate routes [28-31]. With the possible exception of laser trabeculoplasty, current procedures do not attempt to treat the TM. Given that TM degeneration is one of the root causes of IOP elevation in OAG, the development of an efficient way to regenerate the TM could improve IOP control and potentially treat many patients with this disease.

In the present study, we investigated bone marrow (BM) cell injection to promote TM regeneration and reduce the elevated IOP in an animal glaucoma model. We showed that among BM cells, MSC migrated predominantly to the area of tissue damage and were particularly efficient at decreasing IOP, restoring aqueous humor drainage and causing histological tissue repair. Such favorable results were observed although MSC persisted for only a few days, and their effects were replicated through local injection of their secretum. In addition, MSC promoted the reactivation and proliferation of nestin-expressing ocular progenitor cells in the ciliary body which, in turn, persisted in the eye for the duration of the study. Moreover, laser therapy led to both effector cell homing and localized recruitment of endogenous nestin expressing progenitors, thereby opening the door to targeted cell-based therapy of chronic ocular and other disorders.

MATERIAL AND METHODS

Animals

Six to eight week old C57BL/6 male mice and 3-month-old Brown Norway female rats were purchased from Jackson Laboratories (Bar Harbor, ME, USA) and Charles River (Kingston, ON, Can), respectively. Animals were housed in pathogen-free conditions and studied using protocols approved by the Hôpital Maisonneuve-Rosemont (HMR) Research Center Animal Protection Committee.

Isolation, Culture, and Expansion of BMMC

BM was aspirated from femurs and tibias of 2-month-old C57BL/6 mice. BM mononuclear cells (BMMCs) were isolated by using density gradient centrifugation (Ficoll-Paque; Amersham Pharmacia Biotech, Montreal, QC, Can) and suspended in Dulbecco's modified Eagle's medium (DMEM; Gibco, Burlington, ON, Can), 20% heat-inactivated (56ºC, 60 min) fetal bovine serum (FBSI; Hyclone, Logan, UT, USA), 2 μM L-glutamine, 100 U/mL penicillin, and 100 μg/mL streptomycin (Gibco). Cells were plated in 75 cm^2 tissue culture flasks (Sarstedt, Montreal, QC, Can) and incubated at 37°C in 5% CO_2 humidified air. After 48 hours, non-adherent cells were removed, grown until approximately 90% confluence, and then passaged with medium changes every 3-4 days.

MSC characterization

After the second passage, BMMC were characterized for mesenchymal and hematopoietic markers by flow cytometry analysis. The following fluorochrome labeled anti-mouse antibodies were used: CD14- and CD45-APC; CD105-Pacific blue; CD73-PE (all eBioscience, San Diego, CA, USA); and CD90-FITC (BD, Mississauga, ON, Can). Data was collected on a FACS LSRII cytometer (BD) and analysis performed with FlowJo software (Tree Star, Ashland, OR, USA). Cells positive for the hematopoietic marker CD45 were sorted using a FACS Aria III (BD) and both MSC and hematopoietic cells used for *in vivo* experiments. MSC were tested for osteogenic and adipogenic differentiation using osteocyte/chondrocyte or adipocyte differentiation media (Invitrogen, Burlington, ON, Can), and alizarin red S and oil red O staining (Sigma, Oakville, ON, Can), respectively.

Trabecular Meshwork Cell Culture

The TM cell line MUTM-NEI/1 originating from $H2K^b$-tsA48 heterozygote mice (genetic background CBA/ca X C57BL/10) was a kind gift of Dr. Joram Piatigorsky [32]. Cells were cultured in non-permissive conditions (37°C) in 75 cm^2 adherent tissue culture flasks with TM cell medium consisting of Iscove's Modified Dulbecco's Medium (IMDM; Gibco) supplemented with 20% FBSI, and L-glutamine, penicillin and streptomycin at above concentrations.

Co-Culture condition

MSC to TM cell differentiation was assessed in co-culture experiments. Briefly, $1X10^6$ MSC were seeded in a 75 cm^2 tissue culture flask and stained using CellTracker Blue CMAC according to manufacturer's protocol (Invitrogen). Cells were washed with Hanks' medium before adding fresh TM cell culture medium and seeding of $1X10^6$ MUTM-NEI/1 cells at day 0 of co-culture. After 7 days, cells were harvested and expression of TM cell markers was analyzed using flow cytometry. The following unlabeled antibodies were used according to manufacturer's protocol: Rabbit anti-mouse Pax6, aquaporin-1 (both from US Biological; Burlington, ON, Can), laminin (Sigma) and fibronectin (Millipore; Nepean, ON, Can). Primary antibodies were revealed with goat anti-rabbit AlexaFluor488 (Invitrogen).

MSC Culture medium for paracrine studies

MSC secretum was obtained after seeding $1X10^6$ MSC in 15 ml DMEM for 24 hours at 37°C in 5% CO_2 humidified air at either 21% or 5% O_2. MSC conditioned medium (CM) was then harvested and concentrated 40X using 10 kDa centrifugal filter devices (Amicon Ultra-15, Millipore)

Glaucoma Model

To induce ocular hypertension, rats were anesthetized using intraperitoneal injection of ketamine (50 mg/kg; Wyeth; Guelph, ON, Can), and xylazine (2.2 mg/kg; Bayer; Toronto, ON), and drops of the local anesthetic proparacaine (Alcon Canada; Mississauga, ON, Can) were applied to the eyes. The method developed by Levkovitch-Verbin *et al* was modified to selectively damage only half of the circumference of the anterior chamber angle [33]. Briefly, 90 spots of 50 μm diameter were directed towards the nasal 180° of the trabecular

meshwork area using a Coherent Novus Omni laser (Laser Labs Inc; Tampa, FL, USA) set at 532 nm wavelength, 200 mW and 0.1 second duration. Baseline IOP was measured weekly with a Tonopen-XL (Medtronic; Mississauga, ON, Can). IOP was obtained in rats by performing an average of 10 measurements at a time by a blinded observer.

Transplantation

Before injection, cells were stained using carboxyfluorescein succinimidyl ester (CFSE, CellTrace, Invitrogen) dye. A control population was kept *in vitro* in BMMC medium to measure fluorescence changes over time. CFSE stained cells were suspended at $1x10^5$ cells/µl in saline solution (Baxter; Pointe-Claire, QC, Can). Intraocular transplantation was performed during the hour or 4 days following laser treatment. Prior to intraocular injection, ten µl of aqueous humor (AH) was removed from the anterior chamber of the treated eye using a $28^{1/2}$ gauge needle under direct observation with a binocular surgical microscope. Injection of ten µl of cell preparation (cells, saline solution-placebo or MSC-CM) was performed at the same injection site immediately after AH removal and under identical conditions. Injection was carried out over the course of 1 minute to avoid additional stress to the anterior chamber. Although minimal reflux was observed after injection, no leaks were observed beyond the first 24h when using the Seidel test. Rare animals (2 for the duration of the study) have sustained additional damage to the anterior chamber during the injection, and were removed from the experiment. All animals were kept under immunosuppressed conditions by daily intraperitoneal injection of cyclosporine A (Sandimmune; Novartis Pharma, Montreal, QC, Can) starting 3 days before treatment and continued for the duration of the experiment.

Tissue Processing

Animals were euthanized by intraperitoneal injection of pentobarbital sodium (Euthanyl; ***Bimeda-MTC Animal Health,*** Cambridge, ON, Can). Enucleated eyes were embedded in Optimum Cutting Temperature (Tissue-tek O.C.T.; Fisher Scientific, Ottawa, ON, Can) compound and flash-frozen in liquid nitrogen. Twelve µm sections were cut by cryostat (Leica, Richmond Hill, ON, Can) and mounted on slides (Fisher Scientific). After fixation in 4% paraformaldehyde, hematoxylin and eosin staining (Sigma) was used to examine anterior segment histology.

Aqueous humor outflow

To monitor aqueous humor outflow, we relied on a modified methodology from P.L. Kaufman et al [34]. Briefly, 5 µl of C-14 labeled dextran (Dextran [carboxyl-14C] Avg M.W. 70,000, American Radiolabeled Chemicals Inc. St-Louis, MO, USA) was injected on day 8 over the course of one minute in the anterior chamber of rats from laser treated, laser + low oxygen CM treated or untreated groups (n=3 per group). One hour prior to intraocular injection, unlabeled dextran (0.5ml, 100mg/ml, Sigma) was injected intravenously to reduce risk of radiolabeled dextran entrapment in organs. To calculate trabecular outflow, blood samples were taken from a cannula implanted in the jugular vein on the side of the treated eye of anesthetised animals. Blood samples were collected every 2 minutes after dextran C-14 injection to monitor re-entry of the radiolabeled marker to the blood.

EDU labeling

To monitor the fate of anterior chamber cells during tissue regeneration, 9 animals were injected intraperitoneally with 50mg/kg of EDU (Invitrogen) from days 1 to 3 after laser damage and intraocular injections [35].

Immunofluorescence

Samples were incubated for 1 hour with blocking-permeabilizing solution of PBS containing 1 mg/ml bovine serum albumin (BSA; Vector Labs., Burlington, ON, Can) and 1 µl/ml Tween (Sigma). Slides were incubated overnight at 4^oC with unlabeled mouse anti-nestin, rabbit anti-Ki67 (BD) and rabbit anti F4-80 antibodies (abcam, Toronto, ON, Can). Primary antibodies were revealed with goat anti-rabbit AlexaFluor488 and goat anti-mouse

AlexaFluor594 (all from Invitrogen). Nuclei were stained with mounting medium containing DAPI (Vectashield; Vector Labs). EDU labeling was performed with Click-it EDU Alexa Fluor 488 imaging kit (Invitrogen) according to manufacturer's instructions. Histological sections were observed by confocal microscopy (Axiovert 100 LSM 510Meta; Carl Zeiss, Jena, Germany) while fluorescence and surface area of anterior chamber structures were analyzed using AxioVs40 V4.8.2.0 (Carl Zeiss).

Tunnel assay

TUNEL assay was performed using the *In Situ* Cell Death Detection Kit, Fluorescein (Roche) according to the manufacturer's instructions. Briefly, ocular sections were permeabilized in 0.1% Tween for 15 minutes. Sections were than incubated with the enzyme terminal deoxynucleotidyl transferase and fluorescein-conjugated dUTP at 37°C for 1 hour. Nuclear DNA was stained with DAPI (Vector Labs).

Statistical analysis

Comparisons between animal groups were done using two-way ANOVA and Mann-Whitney T test. Statistical analyses were performed using GraphPad Prism version 4.0 (San Diego, CA, USA). All statistical tests were two-sided and performed at the significance level of 0.05.

RESULTS

Animal glaucoma model

In order to study the contribution of MSC to the regeneration of the TM in glaucoma, we opted for a modified version of the laser-induced animal model developed by Levkovitch-Verbin *et al* which allowed for an internal control consisting of an untreated segment within the laser treated eye. Laser treatment covering 180° of the anterior chamber angle resulted in a significant elevation of the IOP, with a peak IOP of 26.9 ± 0.7 mmHg at day 12 (Fig.1A, mean ± SEM; n=10; $p<0.001$), as opposed to healthy control animals with peak IOP of 20.8 ± 0.2 mmHg (Fig. 1A, n=10). Laser induced IOP elevation persisted for a period of approximately 30 days.

Injection of bone marrow cells *in vivo* decreases IOP

We first investigated the ability of cultured BMMCs to promote IOP pressure recovery *in vivo* (Fig. 1A). Increased IOP was observed in all groups on day 2 after laser exposure. While IOP continued to rise in laser treated animals, peaking on day 10, the ocular injection of $1x10^6$ BMMCs rapidly lowered IOP, which returned to baseline significantly earlier (day 8) than in the laser only group (day 32; $p<0.01$). Injection of saline solution resulted in IOP similar to untreated controls. Cellular controls, which consisted of lymphocytes, failed to impact on IOP curves. The nature of injection content had no effect on IOP levels at day 2 for all groups (mean ranging from 26.5 to 27.7 in all 4 groups). However, the time required for BMMC to reduce the mean IOP by 50% was 4.3 days, 5 times faster than the time required to obtain the same pressure drop in the laser only (20.5 days), saline (22.5 days) or lymphocyte (22.2 days; $p < 0.001$) control groups.

BMMC Characterization

Adherent BMMCs harvested from B6 mice and expanded in culture *in vitro* were tested for hematopoietic markers (CD45 and CD14). After 2 passages, 65% of these adherent cells were negative for CD45 and CD14 (Supplementary Fig. 1A). These cells expressed classical MSC markers: CD73, CD90 and CD105 (Supplementary Fig. 1B-D), and were capable of adipogenic and osteogenic differentiation in the proper media, thus satisfying MSC criteria (Supplementary Fig. 1E-F). To determine which of hematopoietic cells [36] or MSC mediated the IOP drop, BMMC were sorted according to CD45 expression and injected *in vivo* (Fig. 1B). Both hematopoietic (CD45+) and MSC groups were injected the same number of cells ($5X10^5$ cells) corresponding approximately to that found in the total BMMC population. Laser only animals had a peak IOP of 26.8 ± 0.7 mmHg on day 6 and those injected with CD45+ cells

peaked at 25.6 ± 0.6 mmHg on day 12. In contrast, the MSC group demonstrated a rapid fall in IOP on day 5 (21.6 ± 0.7 mmHg; *n*=9; $p<0.01$). The time required to reduce the pressure by 50% was 4.5 days, 6 times faster than the time required to obtain the same drop in the laser control (27.8 days) or CD45+ cells (26 days; $p < 0.001$). Additionally, cumulative IOP was significantly lower in groups treated with MSC ($p<0.01$ for BMMC and $p<0.001$ for MSC) than in the other injection control groups (Fig. 1C). Thus, these results indicate that within BMMCs, MSC are primarily responsible for the rapid restoration of baseline IOP.

Injection of MSC *in vivo* restores TM structure

Ocular tissue sections were performed to investigate mechanisms used by MSC to promote healing of anterior chamber angle structures. One week post photocoagulation, anterior chamber angle structures (iris, ciliary body and TM) of damaged eyes showed signs of inflammation, desquamation, and anterior synechiae (Fig. 1E). Cellular composition of these structures at one week depended on the treatment, as pigmented cells were the dominant cell population in the laser only groups, with the additional presence of non-pigmented cells in the MSC-injected laser-treated eyes. One month after photocoagulation, eyes that did not receive MSC transplantation presented scarring in the TM area, as well as invasion by pigmented epithelial cells. In contrast, eyes that received a MSC graft had an angle structure and histology that approximated that of the intact eye. These observations were confirmed by measuring the surface area of the TM area (Fig 1D). After 30 days, no significant changes could be observed between the normal TM surface area and the group that received MSC transplantation, while the group that did not received MSC had a significantly smaller TM surface ($p<0,01$). These results indicate that MSC injection leads to efficient structural recovery of the anterior chamber angle.

MSC do not transdifferentiate into TM cells *in vitro*

To investigate potential differentiation of MSC into TM cells upon exposure to TM cell environment, these two populations were co-cultured *in vitro*. MSC could be tracked using fluorescent dye labeling (CellTracker Blue) and evaluated for the acquisition of TM features by monitoring the surface antigens aquaporin-1, fibronectin and laminin as well as the nuclear transcription factor Pax6, since these molecules ensure the proper development and function of TM cells (Supplementary Fig. 2). All MUTM-NEI/1 TM cells expressed these surface antigens and transcription factor. However, few MSC expressed laminin and aquaporin-1 in normal culture conditions. Expression levels of Pax6 and fibronectin were not found to be significantly different between both cell populations prior to co-culture. After 7 days of co-incubation, the MSC population failed to acquire expression of aquaporin and laminin indicating that direct contact with TM cells did not promote MSC differentiation.

***In vivo* MSCs migration and survival**

To investigate the mechanisms implicated in IOP lowering, we evaluated the ability of MSC to migrate and integrate *in vivo* into the TM. CFSE labeling of MSC on the day of injection enabled their subsequent detection by immunofluorescence. Tissue sections from animals sacrificed at 24, 48 and 96 hours revealed a major decrease in the number of CFSE+ cells over time (Fig. 2). Cells were no longer detectable in the anterior chamber 96 hours after their injection. MSC clearance may be due to ocular microglia phagocytosis, as approximately 1 in 5 CFSE+ cells co-expressed microglia marker F 4/80 on day 2 (Supplementary Fig. 3). CFSE expression of MSC kept *in vitro* in culture medium was detectable by fluorescent microscopy for 7 days (data not shown). Interestingly, 24 hours after MSC administration, a high number (2.2±0.1 $X10^4$) of cells had migrated to the area of laser damage while only half that number (1.2±0.2 $X10^4$; $p<0,01$) was found in the intact area.

Although this proportion was maintained at 48h (1.0 ± 0.2 X$10^4$and 0.5 ± 0.2 X10^4 in the damaged and intact areas, respectively) the difference was no longer found to be significant at that time. These findings demonstrate that MSC have the ability to specifically migrate to the area of laser damage but do not remain in the anterior chamber for a prolonged period of time.

MSC secreted factors influence ocular regeneration

TM regeneration was observed although MSC rapidly cleared out from the chamber angle (96 h), suggesting that these cells are not inducing tissue repair by integrating the TM and directly replacing the damaged cells. This could imply that their effect was instead mediated by secreted factors and by activation of an endogenous repair mechanism. Hypoxia and cytokines produced by immune cells or environing tissue are known to induce changes in MSC secreted factors [37-39]. To determine the implication of such a mechanism, MSC conditioned medium (CM) was harvested after 24 hour *in vitro* culture under either normoxic or low-oxygen conditions. No significant effect on IOP was observed when laser treated animals were injected concentrated (40X) normoxic MSC-CM (Fig. 3A). Interestingly, when concentrated (40X) low-oxygen CM was injected immediately after laser treatment, peak IOP and subsequent measurements were found to be similar to that of the MSC treated group. We tested the robustness of our treatments by delaying the injection of low-oxygen CM, saline solution control and MSC until 4 days after laser exposure to allow damage and inflammation to develop further in the anterior chamber (Fig. 3B). Again MSC and low-oxygen CM groups induced similar decreases in IOP while saline solution induced no significant improvements. Treatment on day 0 instead of day 4 resulted in lower cumulative IOP for both MSC and low-oxygen MSC-CM ($p<0.05$; Fig. 3C). Histological sections revealed that four days after CM injection, anterior chamber angle tissue structures (iris, ciliary body and TM) showed clear signs of inflammation, desquamation and anterior synechiae (Fig. 3E) Two weeks after photocoagulation, eyes that received normoxic CM treatment still showed considerable signs of scarring. In contrast, eyes that received low-oxygen CM treatment had an angle structure and histology closer to that of the intact eye. These observations were confirmed by measurement of the TM surface area (Fig. 3D). After two weeks, no significant changes could be observed between the normal TM surface area and the group that received low-oxygen CM treatment while the group that received normoxic CM treatment had a significantly smaller TM surface ($p<0,01$).

Additionally, injection of low-oxygen CM restored TM functionality by increasing aqueous humor outflow (Supplementary Fig. 4). Indeed, clearance of the radiolabeled tracer was very low after laser damage when compared to normal controls with an estimated peak clearance of 0.04 ± 0.006 µl/min versus 0.20 ± 0.06 µl/min, respectively ($p<0,05$). Low oxygen-CM groups demonstrated significantly greater humor clearance (0.11 ± 0.003 µl/min, $p<0,05$) than laser treated groups. Overall, these results indicate that cellular stress is required for MSC to secrete therapeutic factors, and that such factors exert a key role in the functional recovery of ocular tissue.

Decreased IOP allows for better survival of retinal cells

To confirm the importance of decreased intraocular pressure for the survival of retinal cells, a TUNEL assay was performed on eyes treated with low-oxygen and normoxic CM (Supplementary Figure 5). After 12 days of sustained IOP, TUNEL-positive apoptotic cells were observed within the retina of all treated eyes but in significantly lower numbers in group treated with low-oxygen CM. These data indicates the importance of IOP drop in retinal cell survival.

MSC trigger the appearance of nestin+ progenitor cells

The outer layer of the ciliary body pigmented epithelium is home to a quiescent neural

progenitor cell (NPC) population that can be detected by expression of the progenitor cell marker nestin [40-46]. As both pigmented and non pigmented cells were observed in the TM area of MSC and MSC-CM treated eyes, we investigated whether these cells could represent neural progenitor cells. Staining for nestin-positive cells was conducted in the chamber angle area: ciliary body, TM and limited portion of the iris (Fig. 4). In an untreated eye, no nestin positive cells were detectable (Fig.7A). Few nestin-positive cells were detected in the laser treated group injected with the lymphocyte control cell population (Fig. 4A). In comparison, a high proportion of nestin-positive cells were observed in the MSC and low-oxygen CM treated groups, and were comprised of both pigmented and non-pigmented cells (Fig. 4B-C). Importantly, all nestin positive cells were found to be endogenous to the eye as the selected antibody was rat specific and nestin expression profiles were identical in eyes treated with MSC and MSC-CM (Fig. 4D).

Nestin expression and cellular proliferation correlates with ocular regeneration

As nestin expression is lost in differentiated neural progenitors and mature cells, we used this marker to investigate progenitor cell evolution during tissue regeneration (Fig. 5 and Supplementary Figure 6). Intact eyes revealed neither cells positive for nestin nor the proliferation nuclear marker Ki67 (with the exception of the corneal surface, which contains replicating (Ki67+) cells). A small number of nestin+ and Ki67 + cells could be observed in laser-treated eyes injected with lymphocyte controls: 2.5% (nestin) and 1% (Ki67) of total cells in the laser damaged area (Fig. 5A-B). Both markers were absent in the intact area of this group. In contrast, an increased number of cells harboring nestin and Ki67 were found in the laser damaged area of MSC treated rats and peaking on day 4 (Fig. 5C-D). Approximately 25% of nestin positive cells co-expressed Ki67 (data not shown). Interestingly, the moment of peak expression for nestin and Ki67 corresponded to the time required to lower IOP by 50% in the MSC and MSC-CM treated groups. Although MSC were found in the intact area of the eye, this region was comprised of a significantly lower number of nestin and Ki67 positive cells than the laser damaged area ($p<0.001$).

In the normoxic CM treated group, we found only a trend for an increased number of nestin positive cells between days 2 and 4 (Fig. 5E-F). In addition, no significant differences in nestin and Ki67 expression were observed between the intact and damaged areas in this group. Nestin and Ki67 expressing cells were significantly more abundant in the low-oxygen CM than in the normoxic CM group ($p<0.01$ and $p<0.05$, respectively; Fig. 5G-H and Supplementary Fig. 6). While the injection of CM should lead to an even distribution of paracrine factors in the anterior chamber aqueous humor, a higher number of nestin+ cells was found in the damaged than the intact area of the low-oxygen CM treated eyes ($p<0.05$). Collectively, these results indicate that MSC and their secretum have a predominant effect on the activation of neural progenitor cells, which primarily occurs in the laser treated area.

Proliferating cells integrate and survive in chamber angle structures.

As both Nestin and Ki67 are transient markers, we investigated the fate of the proliferating cells using EDU staining (Figure 6). In animals treated with low oxygen CM, the peak of proliferation was observed between days 1 and 3, hence, a group of animals was treated by daily intraperitoneal injections of EDU during that time to stain the proliferating cells. A large number of EDU positive cells ($6,4\pm0.4$ $X10^5$; Fig. 6 B-C, J) were found in the damaged area of the treated eyes on day 8. Although these cells decreased significantly ($p<0.001$) when observing treated animals on day 32 ($5,2\pm0.4$ $X10^5$; Fig 6 H-I, J), they were still present in large enough numbers to confirm they successfully implanted in the area of damage. No EDU positive cells were detectable after one month in the intact area (Fig. 6 G). This indicates

that the Ki67+ cells observed between days 1 and 4 remained, a majority of which were nestin+, remained in the chamber angle and fully integrated in the ciliary body and TM.

Laser exposure raises local ocular tissue sensitivity to MSC secretum

In light of the finding that cellular damage promoted local recruitment of progenitor cells, we evaluated whether laser-induced tissue damage had a local or systemic influence on MSC- or MSC-CM-induced progenitor cell recruitment and cellular proliferation. To answer this question, intact and laser-treated eyes were injected with MSC and low-oxygen CM. In an intact eye, no nestin or Ki67 positive cells could be detected after MSC injection (Fig. 7A;C). In contrast, the injection of the same number of cells in a laser damaged eye led to an increase in nestin and Ki67 positive cells which was predominant in the area of laser damage (Fig. 7A;D). In addition, low-oxygen CM increased nestin and Ki67 positive cells diffusely in the anterior chamber of both eyes whether they were laser-treated or not (Fig. 7B;E). Moreover, laser treatment was the only factor causing a differential increase in nestin-expression after CM exposure (Fig. 7B;F; $P<0.01$). These results indicate that laser exposure enhances cellular sensitivity to MSC resulting in targeted NPC generation and cell proliferation. MSC-CM generated increases in nestin and Ki6 positive cells in laser-unexposed eyes or ocular regions, but only laser exposure promoted differential NPC enhancement.

DISCUSSION

While embryonic stem cells have been used to repair damaged ocular tissues, to our knowledge this is the first study to report that bone marrow cell subsets harbor regenerative potential, both functional and histological, for the anterior segment of the eye. We identified MSC as prime mediators of this beneficial effect. In addition, our findings demonstrate the unique ability of paracrine factors secreted by low-oxygen cultured MSCs to enhance the function and stimulate the proliferation of ocular progenitor cells. We also report that local stem cell recruitment in the ocular anterior chamber upon exposure to MSC was associated with functional tissue repair. Moreover, laser-induced endogenous progenitor cell stimulation could explain why very short exposure to MSC or their paracrine factors can repair dysfunctional trabecular meshwork. Such an approach opens the door to cellular therapy in patients with chronic conditions, such as glaucoma.

MSC were found to be the crucial BMMC sub-population inducing a functional regenerative effect and lowering IOP, as ablation of MSC from the injected cells resulted in considerably less efficient tissue repair. Neither injection of saline solution nor lymphocytes could decrease IOP, indicating that IOP drop did not result from non-specific medium or cell injections. In addition, lymphocytes being particularly prone to induce immune reactivity, the fact that their administration failed to decrease IOP suggests that the decreased pressure did not result from an increased inflammatory response to the graft [47-49]. Interestingly, MSC injected in the anterior ocular chamber persisted only for a few days, far less than the 5 weeks persistence in the retina observed after MSC injection in the vitreous in a similar glaucoma model [50]. However, the duration of MSC infiltration of the TM observed in our study is in line with other studies of intra-arterial cell injection in animal models of stroke where MSC persist only transiently and are no longer found after 7 days [5, 51-53]. This could result from MSC escaping from the injected eye through the TM or from early mortality after migrating to areas of severe cellular stress inhospitable to long term engraftment [54]. Our findings suggest that such an environment leads to MSC apoptosis and phagocytosis by ocular microglia. Conversely, the observed beneficial effects indicate that long term engraftment is not required for ocular regeneration and that less than 4 days are sufficient to generate a physiological effect.

The mechanisms by which MSC induce tissue recovery are still widely debated, with cellular differentiation and paracrine effects being the two lead possibilities [8]. Our results clearly favor the latter, as the lack of MSC differentiation *in vitro* upon exposure to TM cells, their early disappearance from the TM *in vivo* as well as the rapid decrease of IOP and rise of aqueous humor clearance within days of low-oxygen MSC-CM injection, all indicate that MSC likely act through the release of soluble mediators. Moreover, the absence of pressure lowering after injection of unstressed MSC-CM reinforces the need for cellular stress to activate MSC [55-62]. These findings provide clear evidence that MSC can act in a paracrine fashion and exert their protective and regenerative effect without the need for prolonged tissue infiltration.

The ciliary body hosts a cell population known to be quiescent neuronal progenitor cells identifiable by the interfilament protein nestin [40-43]. Nestin is commonly used as a neuronal stem/progenitor cells marker and has been observed in a broad range of regenerating tissues after injury [63-65]. Our data clearly indicate that MSC secretum is responsible for the upregulation of nestin, as well as the cellular proliferation marker Ki67 in the TM. The fact that the peak in nestin-positive cells corresponded to the IOP descent implies a role for neural progenitor cells in tissue regeneration or at least identifies these cells as indicators of functional tissue regeneration. Importantly, nestin and Ki67 were expressed only transiently following exposure to MSC and MSC-CM. This is a reassuring finding since uncontrolled cell proliferation could be deleterious, particularly in a closed environment such as the eye. Additionally, cells tagged with EDU during this active proliferation period were present in large numbers in the damaged area 1 month after injury. This indicates that these cells actively take part in tissue remodeling and in functional recovery after regeneration is complete, a phenomenon suggesting that not only tissue protection, but also tissue regeneration is occurring. However, the current model does not allow for longer term studies and it will be interesting to challenge not only the long-term regenerative potential of MSC and MSC-CM, but also long term functionality of the regenerated TM.

The use of 180° laser-induced damage in this animal model, with 180° intact area in the same eye, allowed the precision of MSC-induced regeneration to be revealed with striking accuracy. Indeed, the damaged TM area contained a greater proportion of transplanted MSC compared to intact areas of the same eye, indicating that injected cells migrate preferentially to the site of laser treatment. Laser induced humoral gradients emanating from damaged cells probably contributed to MSC migration, as inflammatory cytokines and chemokines involved in the migration of immune cells toward wound sites are also implicated in MSC mediated chemotaxis [66-68]. In addition, we have observed that nestin and EDU positive cells were increased more efficiently in laser-treated areas. Nevertheless, MSC usage resulted in a more localized effect than MSC-CM, thus implying that MSC might need to be in close contact with damaged cells to upregulate their cytokine production and influence cells in their immediate vicinity. Such cytokine upregulation could result from damaged area hypoxia, and also from contact with inflammatory factors or other cytokines mediating a form of cellular stress. Moreover, soluble mediators from laser-damaged cells could synergize with MSC secretum to upregulate NPC surface receptors enhancing their response. While the administration of MSC can promote the delivery of numerous therapeutic factors under tightly regulated mechanisms, MSC secretum injection may represent a clinical strategy with broad applicability and low potential for toxicity.

The present study has important clinical implications not only for the treatment of acute disorders but also for chronic diseases such as glaucoma. Indeed, one could envision that laser trabeculoplasty, a standard clinical treatment for

glaucoma, could be combined with MSC or MSC-CM administration to promote TM regeneration in glaucoma patients. Laser trabeculoplasty would have the advantage of generating local damage and inflammation within the TM architecture necessary for MSC activation, although it does not induce the same degree of inflammation or tissue architectural changes as in our model. It might also remove non- or dysfunctional TM cells thus creating space for new TM cells. By promoting preferential homing of MSC to the TM, laser therapy would enable them to enhance nestin-positive stem cell recruitment to replace / repair damaged tissues. However it remains to be determined whether the lower treatment intensity of laser trabeculoplasty and human MSC would yield the same results in humans as the currently investigated treatment conditions. The fact that neuronal progenitor cells can be found throughout the CNS, and that MSC or their secretum can rapidly recruit neural progenitor cells could therefore have implications in the treatment of neurodegenerative disorders outside the eye.

ACKNOWLEDGMENTS

The authors wish to thank Dr Leonard Levin and Dr Nicolas Noiseux for their helpful discussions on the manuscript, Dr. Guy Allaire for his expert input on the ocular histology and Dr Gilbert Bernier for his expertise on ocular progenitor cells.

REFERENCES

1. Wu Y, Chen L, Scott PG, et al. Mesenchymal stem cells enhance wound healing through differentiation and angiogenesis. Stem cells. 2007;25:2648-2659.
2. Li H, Fu X, Ouyang Y, et al. Adult bone-marrow-derived mesenchymal stem cells contribute to wound healing of skin appendages. Cell and tissue research. 2006;326:725-736.
3. Mellough CB, Sernagor E, Moreno-Gimeno I, et al. Efficient stage-specific differentiation of human pluripotent stem cells toward retinal photoreceptor cells. Stem cells. 2012;30:673-686.
4. Fujimoto Y, Abematsu M, Falk A, et al. Treatment of a mouse model of spinal cord injury by transplantation of human induced pluripotent stem cell-derived long-term self-renewing neuroepithelial-like stem cells. Stem cells. 2012;30:1163-1173.
5. Gnecchi M, Zhang Z, Ni A, et al. Paracrine mechanisms in adult stem cell signaling and therapy. Circulation research. 2008;103:1204-1219.
6. Munoz JR, Stoutenger BR, Robinson AP, et al. Human stem/progenitor cells from bone marrow promote neurogenesis of endogenous neural stem cells in the hippocampus of mice. Proceedings of the National Academy of Sciences of the United States of America. 2005;102:18171-18176.
7. Nguyen BK, Maltais S, Perrault LP, et al. Improved function and myocardial repair of infarcted heart by intracoronary injection of mesenchymal stem cell-derived growth factors. Journal of cardiovascular translational research. 2010;3:547-558.
8. Phinney DG, Prockop DJ. Concise review: mesenchymal stem/multipotent stromal cells: the state of transdifferentiation and modes of tissue repair--current views. Stem cells. 2007;25:2896-2902.
9. Uccelli A, Moretta L, Pistoia V. Mesenchymal stem cells in health and disease. Nature reviews. Immunology. 2008;8:726-736.
10. van Haaften T, Byrne R, Bonnet S, et al. Airway delivery of mesenchymal stem cells prevents arrested alveolar growth in neonatal lung injury in rats. American journal of respiratory and critical care medicine. 2009;180:1131-1142.
11. Le Blanc K, Rasmusson I, Sundberg B, et al. Treatment of severe acute graft-versus-host disease with third party haploidentical mesenchymal stem cells. Lancet. 2004;363:1439-1441.
12. Pittenger MF, Martin BJ. Mesenchymal stem cells and their potential as cardiac therapeutics. Circulation research. 2004;95:9-20.
13. Takahashi M, Li TS, Suzuki R, et al. Cytokines produced by bone marrow cells can contribute to functional improvement of the infarcted heart by protecting cardiomyocytes from ischemic injury. American journal of physiology. Heart and circulatory physiology. 2006;291:H886-893.
14. Togel F, Hu Z, Weiss K, et al. Administered mesenchymal stem cells protect against ischemic acute renal failure through differentiation-independent mechanisms. American journal of physiology. Renal physiology. 2005;289:F31-42.
15. Ninichuk V, Gross O, Segerer S, et al. Multipotent mesenchymal stem cells reduce interstitial fibrosis but do not delay progression of chronic kidney disease in

collagen4A3-deficient mice. Kidney international. 2006;70:121-129.
16. Wang W, Jiang Q, Zhang H, et al. Intravenous administration of bone marrow mesenchymal stromal cells is safe for the lung in a chronic myocardial infarction model. Regenerative medicine. 2011;6:179-190.
17. Levin LA, Ritch R, Richards JE, et al. Stem cell therapy for ocular disorders. Arch Ophthalmol. 2004;122:621-627.
18. Quigley HA. Open-angle glaucoma. The New England journal of medicine. 1993;328:1097-1106.
19. Acott TS, Kelley MJ. Extracellular matrix in the trabecular meshwork. Experimental eye research. 2008;86:543-561.
20. Alvarado J, Murphy C, Polansky J, et al. Age-related changes in trabecular meshwork cellularity. Investigative ophthalmology & visual science. 1981;21:714-727.
21. Baleriola J, Garcia-Feijoo J, Martinez-de-la-Casa JM, et al. Apoptosis in the trabecular meshwork of glaucomatous patients. Molecular vision. 2008;14:1513-1516.
22. Caballero M, Liton PB, Epstein DL, et al. Proteasome inhibition by chronic oxidative stress in human trabecular meshwork cells. Biochemical and biophysical research communications. 2003;308:346-352.
23. Grierson I, Howes RC. Age-related depletion of the cell population in the human trabecular meshwork. Eye. 1987;1 (Pt 2):204-210.
24. Tamm ER. The trabecular meshwork outflow pathways: structural and functional aspects. Experimental eye research. 2009;88:648-655.
25. Tamm ER, Fuchshofer R. What increases outflow resistance in primary open-angle glaucoma? Survey of ophthalmology. 2007;52 Suppl 2:S101-104.
26. Kwon YH, Fingert JH, Kuehn MH, et al. Primary open-angle glaucoma. The New England journal of medicine. 2009;360:1113-1124.
27. Chauhan BC, Mikelberg FS, Artes PH, et al. Canadian Glaucoma Study: 3. Impact of risk factors and intraocular pressure reduction on the rates of visual field change. Arch Ophthalmol. 2010;128:1249-1255.
28. Leske MC, Wu SY, Hennis A, et al. Risk factors for incident open-angle glaucoma: the Barbados Eye Studies. Ophthalmology. 2008;115:85-93.
29. Leske MC, Wu SY, Honkanen R, et al. Nine-year incidence of open-angle glaucoma in the Barbados Eye Studies. Ophthalmology. 2007;114:1058-1064.
30. McKinnon SJ, Goldberg LD, Peeples P, et al. Current management of glaucoma and the need for complete therapy. The American journal of managed care. 2008;14:S20-27.
31. Robert MC, Hamel P, Blondeau P, et al. Persistent Leak After Glaucoma Aqueous Shunt Implantation. Journal of glaucoma. 2012.
32. Tamm ER, Russell P, Piatigorsky J. Development of characterization of a immortal and differentiated murine trabecular meshwork cell line. Investigative ophthalmology & visual science. 1999;40:1392-1403.
33. Levkovitch-Verbin H, Quigley HA, Martin KR, et al. Translimbal laser photocoagulation to the trabecular meshwork as a model of glaucoma in rats. Investigative ophthalmology & visual science. 2002;43:402-410.
34. Gabelt BT, Seeman JL, Podos SM, et al. Aqueous humor dynamics in monkeys after topical 8-iso PGE(2). Invest Ophthalmol Vis Sci. 2004;45:892-899.
35. Shruster A, Ben-Zur T, Melamed E, et al. Wnt signaling enhances neurogenesis and improves neurological function after focal ischemic injury. PloS one. 2012;7:e40843.
36. Mansour S, Roy DC, Bouchard V, et al. COMPARE-AMI trial: comparison of intracoronary injection of CD133+ bone marrow stem cells to placebo in patients after acute myocardial infarction and left ventricular dysfunction: study rationale and design. Journal of cardiovascular translational research. 2010;3:153-159.
37. Herrmann JL, Wang Y, Abarbanell AM, et al. Preconditioning mesenchymal stem cells with transforming growth factor-alpha improves mesenchymal stem cell-mediated cardioprotection. Shock. 2010;33:24-30.
38. Rosova I, Dao M, Capoccia B, et al. Hypoxic preconditioning results in increased motility and improved therapeutic potential of human mesenchymal stem cells. Stem cells. 2008;26:2173-2182.
39. Trivedi P, Tray N, Nguyen T, et al. Mesenchymal stem cell therapy for treatment of cardiovascular disease: helping people sooner or later. Stem cells and development. 2010;19:1109-1120.
40. Abdouh M, Bernier G. In vivo reactivation of a quiescent cell population located in the ocular ciliary body of adult mammals. Experimental eye research. 2006;83:153-164.
41. Bhatia B, Singhal S, Lawrence JM, et al. Distribution of Muller stem cells within the neural retina: evidence for the existence of a ciliary margin-like zone in the adult human eye. Experimental eye research. 2009;89:373-382.
42. London A, Itskovich E, Benhar I, et al. Neuroprotection and progenitor cell renewal in the injured adult murine retina requires healing monocyte-derived macrophages. The Journal of experimental medicine. 2011;208:23-39.
43. Martinez-Navarrete GC, Angulo A, Martin-Nieto J, et al. Gradual morphogenesis of retinal neurons in the peripheral retinal margin of adult monkeys and humans. The Journal of comparative neurology. 2008;511:557-580.
44. MacNeil A, Pearson RA, MacLaren RE, et al. Comparative analysis of progenitor cells isolated from the iris, pars plana, and ciliary body of the adult porcine eye. Stem cells. 2007;25:2430-2438.

45. Ohta K, Ito A, Tanaka H. Neuronal stem/progenitor cells in the vertebrate eye. Development, growth & differentiation. 2008;50:253-259.
46. Xu H, Sta Iglesia DD, Kielczewski JL, et al. Characteristics of progenitor cells derived from adult ciliary body in mouse, rat, and human eyes. Investigative ophthalmology & visual science. 2007;48:1674-1682.
47. de Smet MD, Gunning F, Feenstra R. The surgical management of chronic hypotony due to uveitis. Eye. 2005;19:60-64.
48. Willermain F, Rosenbaum JT, Bodaghi B, et al. Interplay between innate and adaptive immunity in the development of non-infectious uveitis. Progress in retinal and eye research. 2012;31:182-194.
49. Kerr EC, Copland DA, Dick AD, et al. The dynamics of leukocyte infiltration in experimental autoimmune uveoretinitis. Progress in retinal and eye research. 2008;27:527-535.
50. Johnson TV, Bull ND, Hunt DP, et al. Neuroprotective effects of intravitreal mesenchymal stem cell transplantation in experimental glaucoma. Investigative ophthalmology & visual science. 2010;51:2051-2059.
51. Duffield JS, Park KM, Hsiao LL, et al. Restoration of tubular epithelial cells during repair of the postischemic kidney occurs independently of bone marrow-derived stem cells. The Journal of clinical investigation. 2005;115:1743-1755.
52. Gnecchi M, He H, Noiseux N, et al. Evidence supporting paracrine hypothesis for Akt-modified mesenchymal stem cell-mediated cardiac protection and functional improvement. FASEB journal; official publication of the Federation of American Societies for Experimental Biology. 2006;20:661-669.
53. Noiseux N, Gnecchi M, Lopez-Ilasaca M, et al. Mesenchymal stem cells overexpressing Akt dramatically repair infarcted myocardium and improve cardiac function despite infrequent cellular fusion or differentiation. Molecular therapy; the journal of the American Society of Gene Therapy. 2006;14:840-850.
54. Copland IB, Galipeau J. Death and inflammation following somatic cell transplantation. Seminars in immunopathology. 2011;33:535-550.
55. Aggarwal S, Pittenger MF. Human mesenchymal stem cells modulate allogeneic immune cell responses. Blood. 2005;105:1815-1822.
56. Block GJ, Ohkouchi S, Fung F, et al. Multipotent stromal cells are activated to reduce apoptosis in part by upregulation and secretion of stanniocalcin-1. Stem cells. 2009;27:670-681.
57. Djouad F, Bouffi C, Ghannam S, et al. Mesenchymal stem cells: innovative therapeutic tools for rheumatic diseases. Nature reviews. Rheumatology. 2009;5:392-399.
58. Groh ME, Maitra B, Szekely E, et al. Human mesenchymal stem cells require monocyte-mediated activation to suppress alloreactive T cells. Experimental hematology. 2005;33:928-934.
59. Hatzistergos KE, Quevedo H, Oskouei BN, et al. Bone marrow mesenchymal stem cells stimulate cardiac stem cell proliferation and differentiation. Circulation research. 2010;107:913-922.
60. Nagaya N, Fujii T, Iwase T, et al. Intravenous administration of mesenchymal stem cells improves cardiac function in rats with acute myocardial infarction through angiogenesis and myogenesis. American journal of physiology. Heart and circulatory physiology. 2004;287:H2670-2676.
61. Uccelli A, Prockop DJ. Why should mesenchymal stem cells (MSCs) cure autoimmune diseases? Current opinion in immunology. 2010;22:768-774.
62. Li L, Zhang S, Zhang Y, et al. Paracrine action mediate the antifibrotic effect of transplanted mesenchymal stem cells in a rat model of global heart failure. Molecular biology reports. 2009;36:725-731.
63. Beguin PC, El-Helou V, Gillis MA, et al. Nestin (+) stem cells independently contribute to neural remodelling of the ischemic heart. Journal of cellular physiology. 2011;226:1157-1165.
64. Bhatia B, Jayaram H, Singhal S, et al. Differences between the neurogenic and proliferative abilities of Muller glia with stem cell characteristics and the ciliary epithelium from the adult human eye. Experimental eye research. 2011;93:852-861.
65. Wiese C, Rolletschek A, Kania G, et al. Nestin expression--a property of multi-lineage progenitor cells? Cellular and molecular life sciences; CMLS. 2004;61:2510-2522.
66. Bocker W, Docheva D, Prall WC, et al. IKK-2 is required for TNF-alpha-induced invasion and proliferation of human mesenchymal stem cells. Journal of molecular medicine. 2008;86:1183-1192.
67. Liu ZJ, Zhuge Y, Velazquez OC. Trafficking and differentiation of mesenchymal stem cells. Journal of cellular biochemistry. 2009;106:984-991.
68. Zhang M, Mal N, Kiedrowski M, et al. SDF-1 expression by mesenchymal stem cells results in trophic support of cardiac myocytes after myocardial infarction. FASEB journal; official publication of the Federation of American Societies for Experimental Biology. 2007;21:3197-3207.

See www.StemCells.com for supporting information available online.

Figure 1. MSC induce a rapid return to normal IOP levels in experimental glaucoma. A) Ocular anterior chambers were either injected with $1X10^6$ BMMC (red), $1X10^6$ lymphocytes (black), saline (green), or received no additional treatment (blue). The grey area represents IOP normal range. IOP was reported as mean±SEM of 4 experiments evaluating 12 animals per group. **B)** $0.5X10^6$ CD45 + cells (black) or $0.5X10^6$ MSC (red line) were injected intraocularly after laser exposure and evaluated as described above. Mean±SEM of 3 experiments evaluating 9 animals per group. **C)** Cumulative IOP exposure in eyes that received laser damage and injection of different cellular populations and controls. Calculated as the integral of IOP over the 4-week experimental period. **D)** TM Cross section area measurements in μm^2. TM surface area was measured for each experimental control (red - laser+MSC group; green - laser+lymphocyte group) and compared to the surface area of a normal TM (grey) **E)** Representative images of hematoxylin-eosin (HE) staining of rat ocular anterior segment before (C: control) and 1 week after laser exposure alone or followed by MSC injection, as well as 4 weeks after laser damage alone or followed by MSC injection. CB: ciliary body; Co: Cornea; I: Iris; TM: Trabecular meshwork. Significance compared to laser control group: *p<0.05, **p<0.01, ***p<0.001. Scale bar = 50 µm

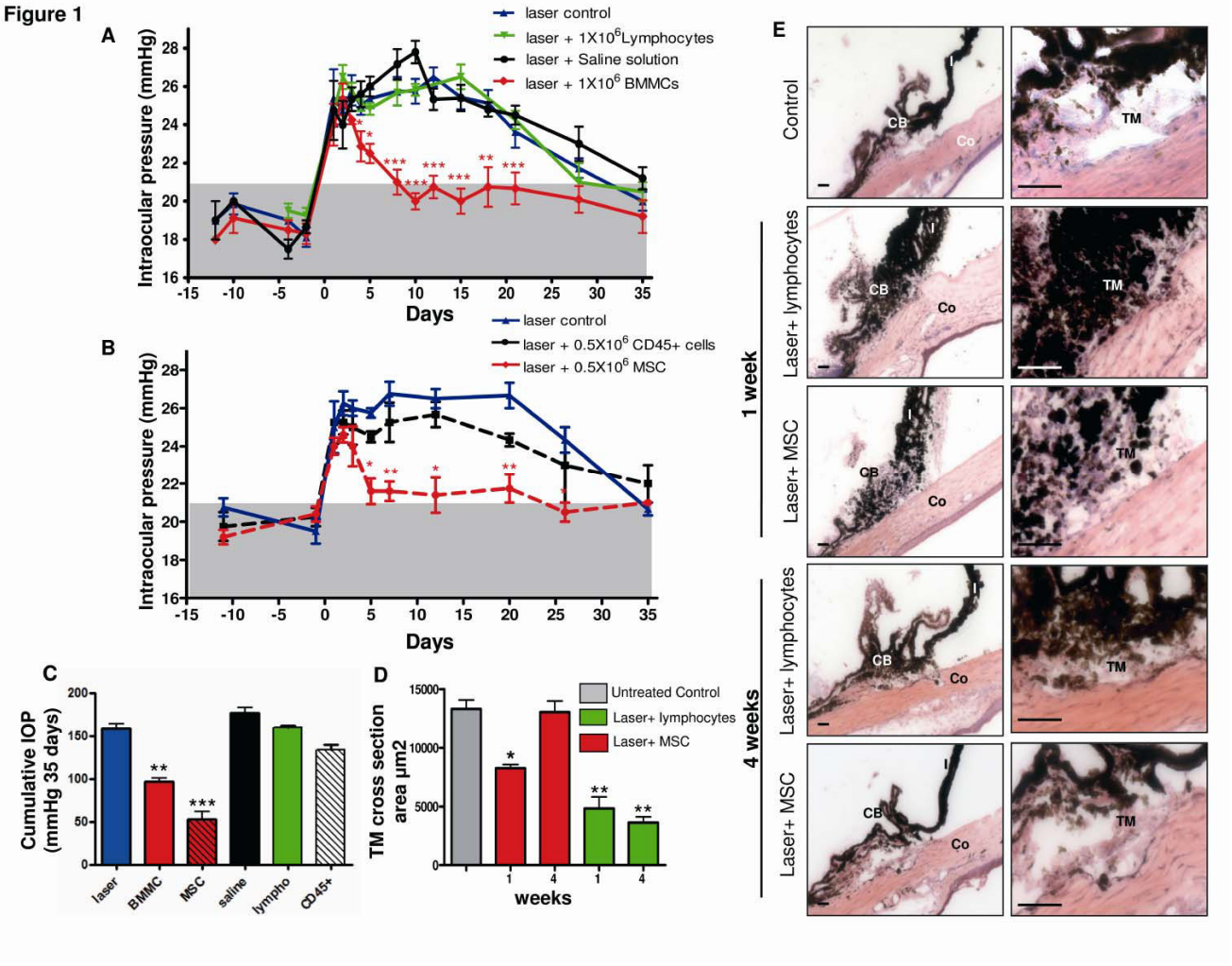

Figure 2. *In vivo* MSCs migration and survival. CFSE-stained MSC were injected in the anterior chamber and tracked *in vivo*. **A-F)** Representative images of the intact (A,C,E) and laser damaged (B,D,F) chamber angles are shown at 24, 48 and 96 hours, respectively, after laser damage and cell injection. Nuclei were DAPI stained. **G)** Compilation of total number of CFSE+ cells present in the eye at 24, 48 and 96 hours after cell injection. Cell numbers (mean±SEM) were determined by fluorescence microscopy analysis of sequential ocular sections (n=5 per time point). Percentages of residual cells are indicated according to the number of injected MSC. **H)** Distribution of CFSE+ cells to the intact or damaged area was measured at each time-point. AC: Anterior Chamber; Cb: cilliary body; Co: Cornea; I: Iris; L: Lens; Arrow: TM. Significance: ***p<0.001. Scale bar = 50 µm

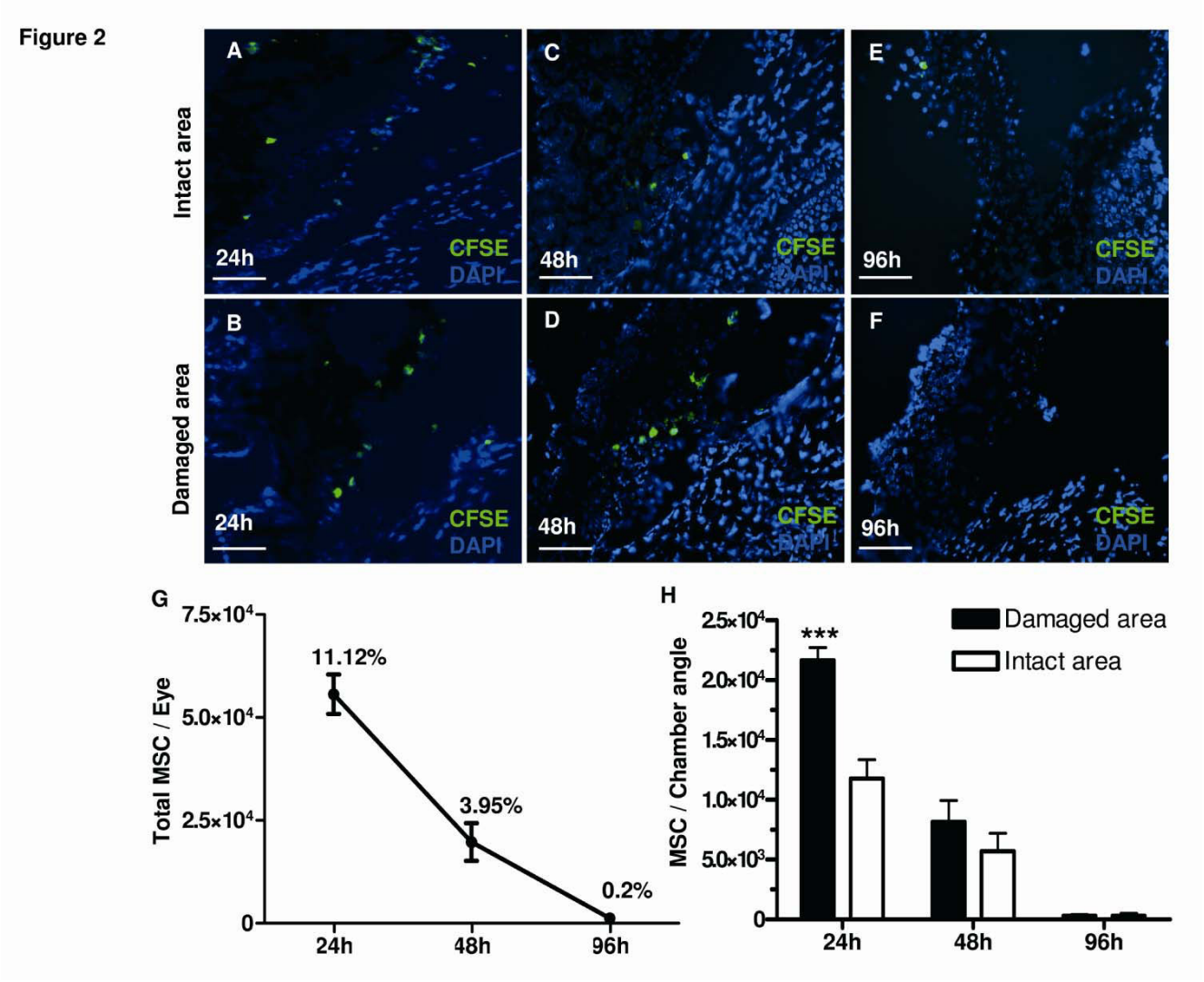

Figure 3. MSC secreted factors promote ocular regeneration. IOP was measured in animals exposed to laser treatment alone (blue) and with injection of MSC (red), saline solution (orange) or MSC-CM generated in normoxic (black) or low-oxygen (green) conditions. MSC-CM was injected either **A)** immediately (day 0) or **B)** 4 days after laser damage. The grey area represents the normal range of IOP. Black vertical lines correspond to the time of laser treatment, and black arrowhead to the time of injection of MSC or their CM. Results expressed as mean±SEM of 3 independent experiments, each with 3 animals per group. **C)** Cumulative IOP exposure in eyes that received laser damage and injection of different cellular populations and controls. Calculated as the integral of IOP over the 3-week experimental period. D) TM Cross section area measurements in μm^2. TM surface area was measured for each experimental control (red - laser+MSC group; green - laser+lymphocyte group) and compared to the surface area of a normal TM (grey) **E)** Anterior ocular segments from rats treated immediately following laser exposure with normoxic or low-oxygen MSC-CM were stained with hematoxylin-eosin (HE). Evaluations were performed at day 4 and 14 after MSC-CM injection. Cb: ciliary body; Co: Cornea; I: Iris. Significance compared to laser control group: *p<0.05, **p<0.01, ***p<0.001. Scale bar = 50 µm

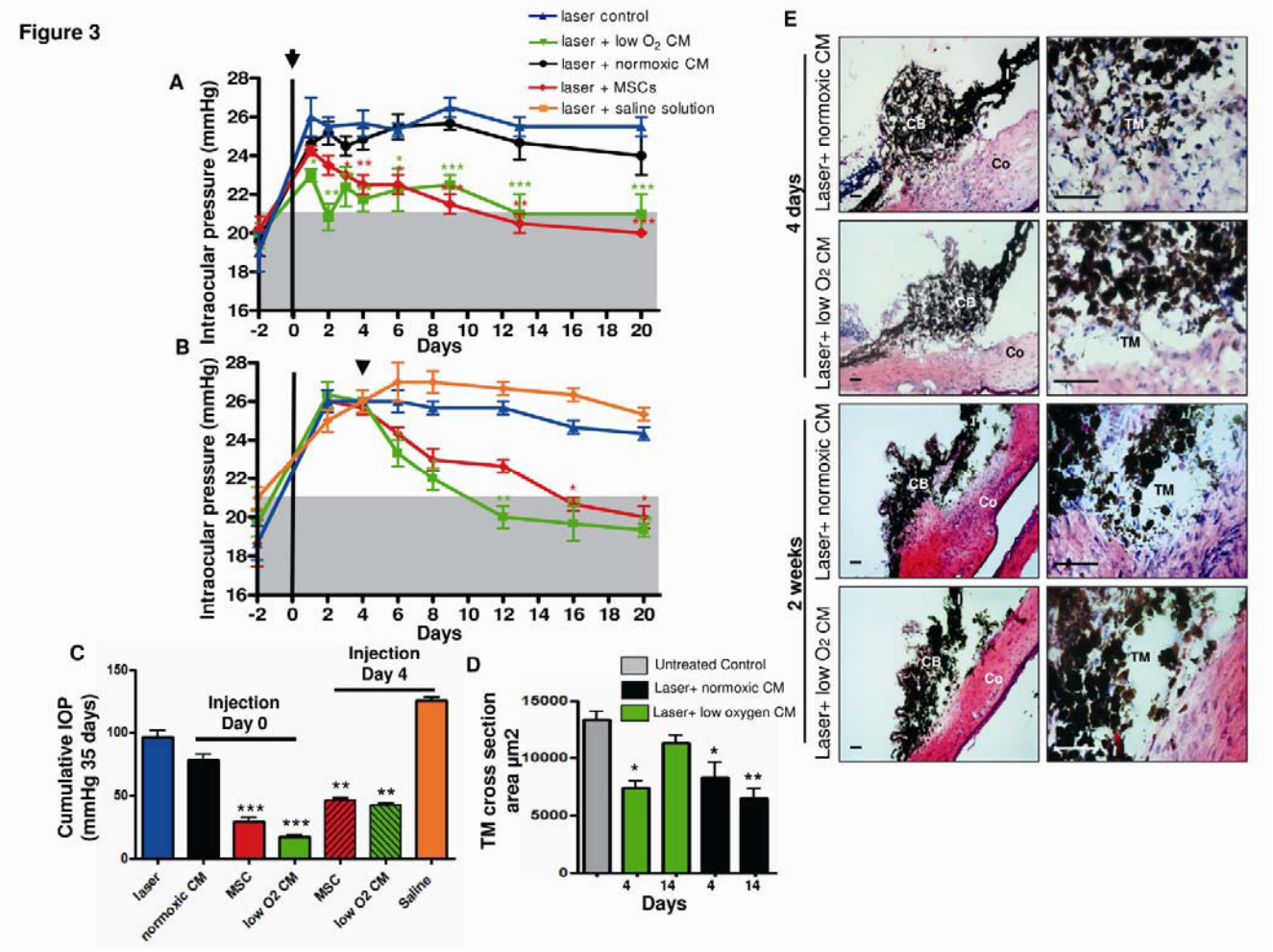

Figure 4. MSC trigger appearance of nestin+ cells. A-C) Light microscopy and immunofluorescence images of TM area from ocular sections of laser treated animals injected with A) lymphocyte controls, B) $0.5X10^6$ MSC or C) low-oxygen MSC-CM and evaluated for stem/progenitor cells using nestin. Nestin+ cells were identified at day 2 after laser treatment and co-localized with pigmented (darkened areas under light microscopy) and non pigmented cells. **D)** CFSE-stained MSC (green) injected at day 0 in laser treated animals were evaluated on day 2 to measure co-expression of nestin (red) with and without DAPI nuclear staining (blue). Scale bar = 50 μm

Figure 4

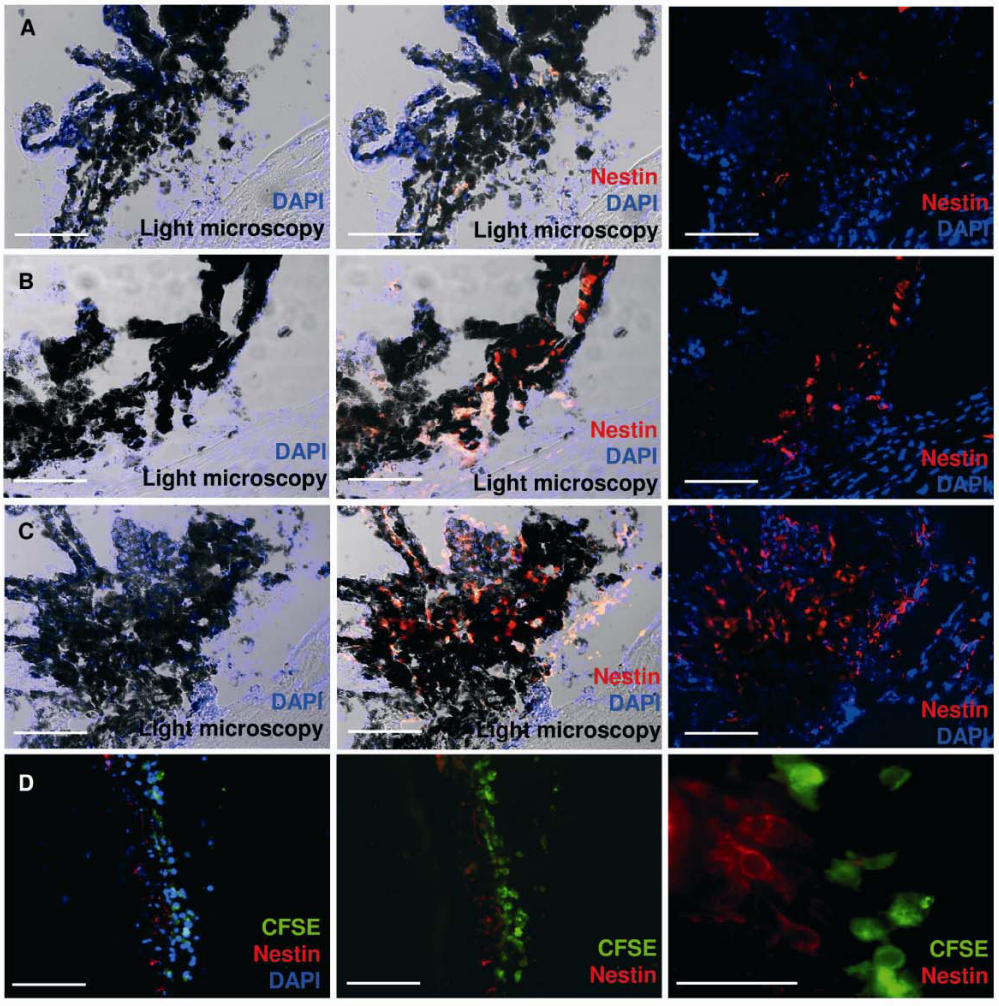

Figure 5. Nestin expression and cellular proliferation correlates with ocular regeneration. Graphs represent compilation of nestin and Ki67 expressing cells in both the intact and damaged chamber angles based on the treatment received: **A)** laser treated eye with lymphocyte control injection, **C)** laser treated eye with MSC injection, **E)** laser treated eye with normoxic CM injection, **G)** laser treated eye with low-oxygen CM injection. Three animals per group from 2 separate experiments (N=6). Numbers indicate the percentage of positive cells found in the area composed of the ciliary body, the TM and a limited portion of the iris. Immunofluorescence histological sections from a rat eye were stained for nestin and Ki67 **(B-D-F-H)**. Pictures are representative images of each group at the time point of peak nestin expression. Nestin (red) Ki67 (green) and Dapi (blue). Significance comparing damaged to intact areas: *p<0.05, ***p<0.001. Scale bar = 100 μm

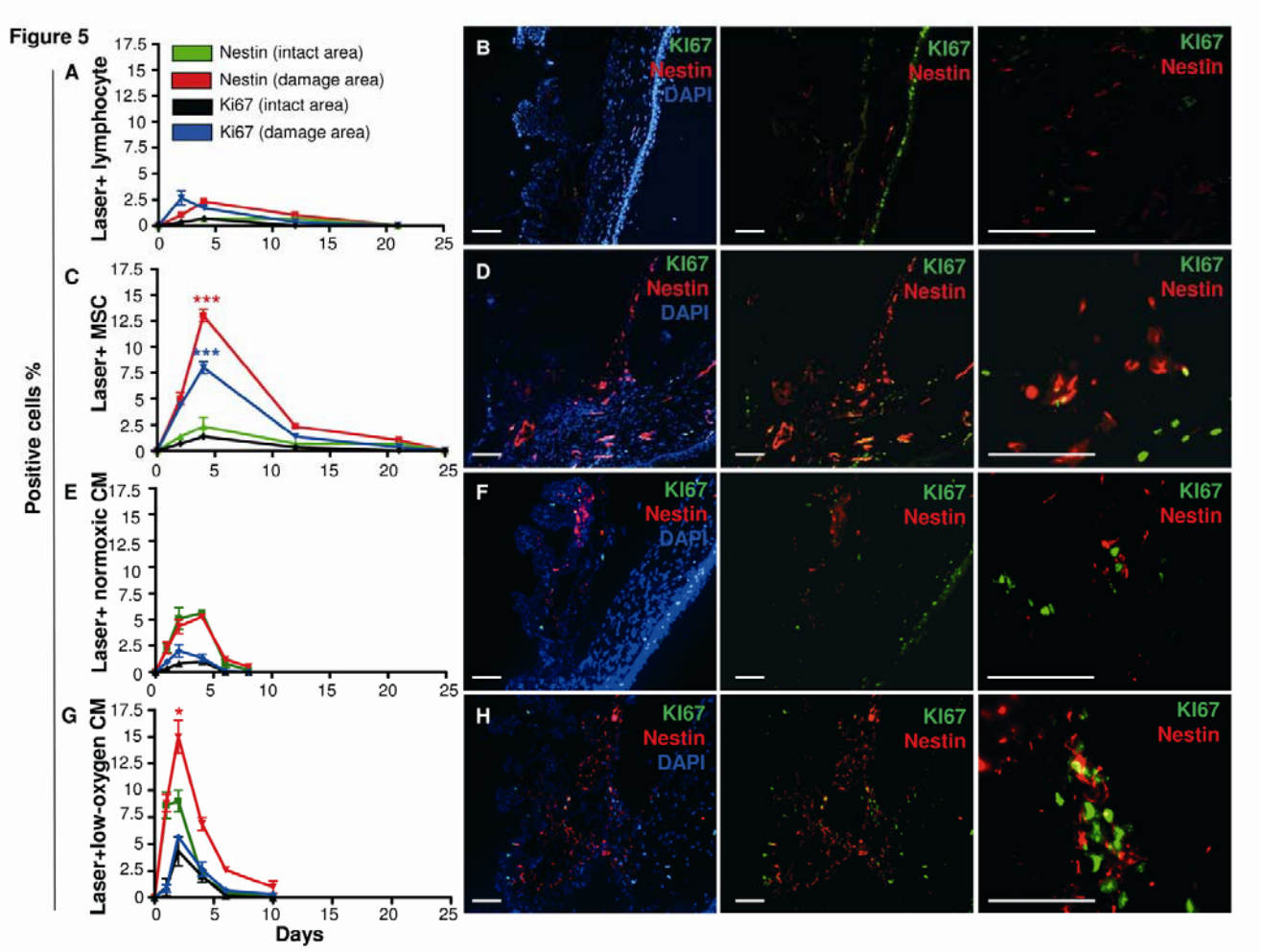

Figure 6. Proliferating cells integrate chamber angle structures. Rats were treated with EDU to observe the replicating cells fate. **A-I)** Representative images of the intact (A,D,G) and laser damaged (B-C,E-F,H-I) chamber angles are shown at day 8, 16 and 32, both as immunofluorescence and light microscopy images, after laser damage and cell injection. Nuclei were DAPI stained. **J)** Compilation of total number of EDU+ cells present in the eye at days 8, 16 and 32 after laser damage and low-oxygen CM injection. Cell numbers (mean±SEM) were determined by fluorescence microscopy analysis of sequential ocular sections (n=3 per time point). Scale bar = 100 μm

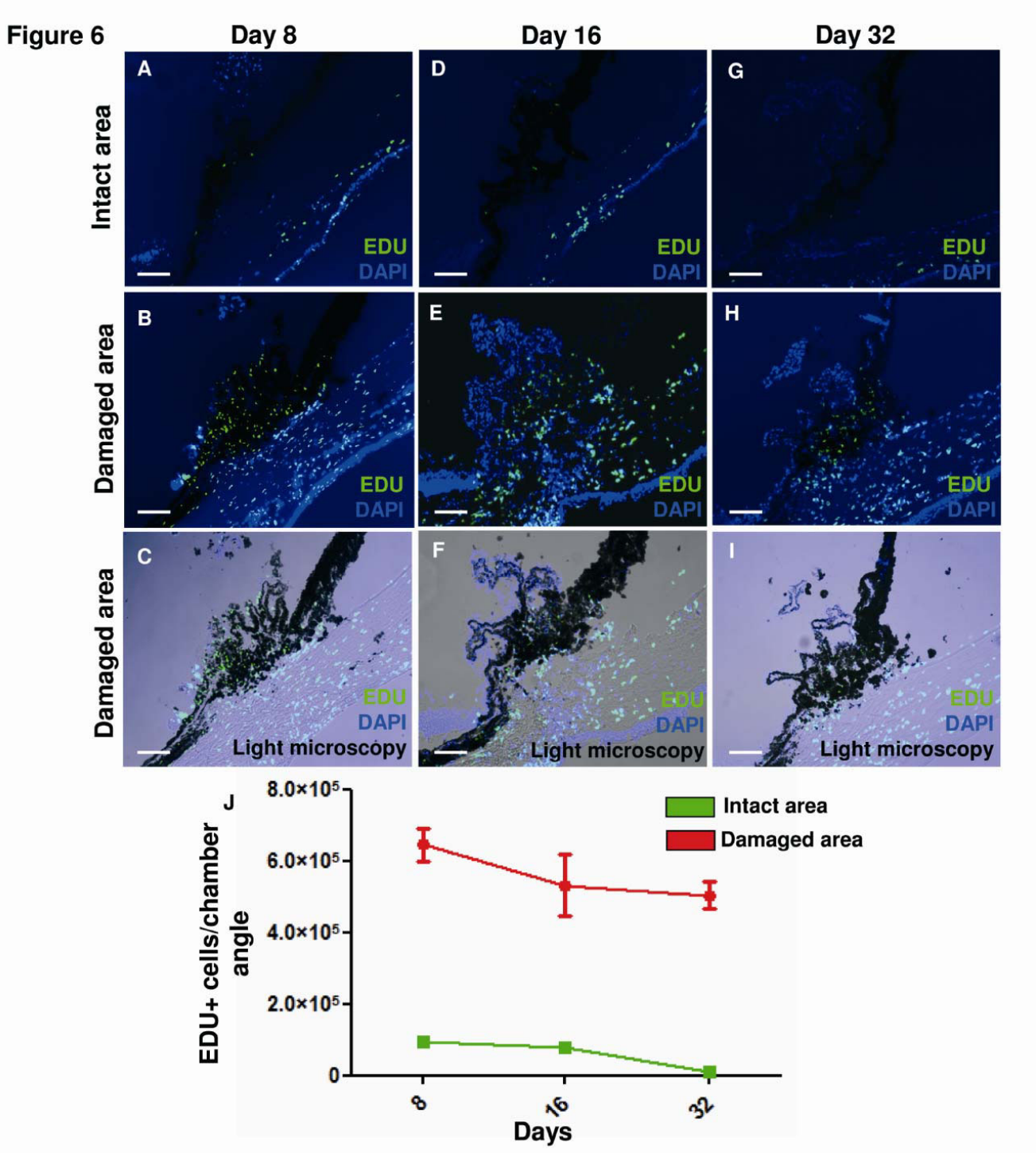

Figure 7. Cellular damage raises ocular tissue sensitivity to MSC secretum. Bar graphs are compilations of nestin and Ki67 positive cells after **A)** MSC injection or **B)** Low-oxygen CM injection. Areas observed were both the temporal (checkered red) and nasal (checkered blue) sides of an intact eye or the damaged (red) and intact (blue) areas of a laser treated eye. Pictures are representative images of each group in both the damaged and the intact area: **C)** Intact eye with MSC injection, **D)** Damaged eye with MSC injection, **E)** Intact eye with Low-oxygen CM injection, **F)** Damaged eye with low-oxygen CM injection. Nestin (red) Ki67 (green) and Dapi (blue). Significance: **p<0.01, ***p<0.001. Scale bar = 100 μm